Journal of Power Sources 183 (2008) 55–61

Contents lists available at ScienceDirect

Journal of Power Sources

journal homepage: www.elsevier.com/locate/jpowsour

Electrochemical parameter identification—An efficient method for fuel cell impedance characterisation

Michael A. Danzer*, Eberhard P. Hofer

Albert-Einstein-Allee 41, 89081 Ulm, Germany

ARTICLE INFO

Article history:
Received 31 January 2008
Received in revised form 11 April 2008
Accepted 27 April 2008
Available online 4 May 2008

Keywords:
Fuel cell
Impedance
Parameter identification
Impedance spectroscopy

ABSTRACT

Electrochemical parameter identification (EPI) is a novel, application-oriented characterisation method for fuel cell impedances. EPI strictly works in the time domain, with a model of the fuel cell impedance and measurements of the excitation and the response in the time domain. This approach reduces the measurement time considerably in comparison to frequency domain measurements for electrochemical impedance spectroscopy. The use of a superimposed signal as system excitation leads to less interference of the fuel cell operation than a current interrupt. Short measurement time and little interference enable an online application of the method during the operation of the fuel cell. A simple discrete-time model describing the dynamic electrical behaviour of the fuel cell is depicted as an equivalent circuit which consists of a voltage source and the impedance as internal resistance. The model parameters are identified by a hybrid optimisation algorithm using the sampled excitation and response signals. A comparison of measured impedance spectra at various operation conditions with impedance models identified by EPI shows very good agreement over a wide frequency range and emphasizes the reliability of EPI.

1. Introduction

For both the development and the operation of fuel cells information on the electrochemical behaviour and on the internal states of the fuel cell stack is needed. The operator asks if the membrane is sufficiently humidified, if the gas diffusion layer is flooded and how losses can be minimised. The control engineer is interested in the dynamics of the power source to apply dynamic load changes. The developer wants to validate the quality of the membrane, the contact, and charge transfer resistances. An approach which gives an insight in the fuel cell stack is the analysis and identification of the fuel cell impedance [1]. The impedance of a fuel cell incorporates detailed information on the intrinsic loss factors, on the conductivity of the membrane, on the electrode processes, and kinetic losses. As a consequence, an efficient and reliable characterisation method for fuel cell impedances with short required measurement time and little interference is of general interest to both, developers and operators.

The standard characterisation procedure for electrochemical systems is carried out in four steps: apply an electrical stimulus to the analysed system, observe the response, generate a mathematical impedance model or an equivalent circuit, and identify the model parameters [2]. The importance of modelling as an integral part of the investigation is emphasized [3]. Generally, the methods of characterising impedances are subdivided into frequency methods and time domain methods.

Electrochemical impedance spectroscopy (EIS) is an established frequency domain method. The approach of EIS is to measure impedance by applying successively single-frequency currents to the system and measuring the real and imaginary parts of the resulting voltage at that single frequency [2]. Measuring the frequency response yields an impedance spectrum which can be modelled by an equivalent circuit, and identified by nonlinear complex parameter identification. The prerequisites for good impedance spectra, the Kramer–Kronig conditions, are linearity, causality, stability, and finiteness of the examined system [4]. Consequently, the recorded impedance spectrum of a nonlinear system, as fuel cells are, is only valid in a neighbourhood of the operating point. The advantage of EIS which is widely used for the characterisation of fuel cell impedances [1,5–8] is that impedance models can be identified with a high accuracy and reliability. The main shortcomings of EIS are the long measurement time and the expensive measuring setup.

The most commonly used time domain method for the characterisation of power sources, especially of fuel cells is the current interrupt (CI) technique [9,10]. At CI the perturbation is an interruption of the current. The resulting transient voltage response

* Corresponding author at: Ulm University, Institute of Measurement, Control and Microtechnology, Albert-Einstein-Allee 41, 89081 Ulm, Germany.
Tel.: +49 7315026325; fax: +49 7315026301.
E-mail addresses: michael.danzer@uni-ulm.de (M.A. Danzer), ep.hofer@uni-ulm.de (E.P. Hofer).

0378-7753/$ – see front matter © 2008 Elsevier B.V. All rights reserved.
doi:10.1016/j.jpowsour.2008.04.071

is observed. In theory, and with a low reliability in practice, the ohmic contribution to the overall impedance can be seen from the height of the rectangular step of the potential [9]. The approach of impedance characterisation using time domain measurements can be improved by transformation of the collected data into frequency domain and subsequent analysis of the resulting frequency-dependent impedance [11]. The advantages of CI in comparison with EIS are that CI needs less measurement time, and that the perturbation can easily be realised with simple power electronics or just with a switch [10]. The main drawback is that CI interferes strongly with the operation of the fuel cell. It should also be noted that an impedance spectrum generated by this method does, strictly speaking, not comply with the Kramer–Kronig conditions. The spectrum is only valid in a neighbourhood of the operating point, but the fuel cell current at CI is changed in between two operating points.

The electrochemical parameter identification (EPI) presented in this work is a model-based method for the characterisation of fuel cell impedances which works strictly in the time domain. Whereas Macdonald claims that "time-varying results are generally Fourier- or Laplace-transformed into the frequency domain, yielding a frequency-dependent impedance" [2], EPI takes the direct way characterising the impedance in the time domain. Instead of transforming the collected data into frequency domain, EPI transforms the complex impedance model into time domain and identifies the impedance parameters directly by using the time domain measurements of the perturbation and the system response. For system perturbation at EPI the fuel cell current is superimposed with a short small signal sequence which is generated based on the sensitivity of the impedance model parameters. A hybrid real-valued optimisation algorithm identifies the parameters of the impedance model. The advantages of EPI in comparison with EIS are the considerably decreased measurement time and the fact that EPI works with standard hardware, without the need of a frequency analyser. In comparison with CI it is expected that EPI reaches a higher accuracy with less interference to the operation of the fuel cell.

2. Impedance characterisation

2.1. Contributions to the fuel cell impedance

Impedance spectra of fuel cell stacks are a superposition of various intrinsic loss factors and transient processes. Or in the words of an electrochemist: "A multitude of fundamental microscopic processes take place throughout the cell when it is electrically stimulated and, in concert, lead to the overall electrical response" [2]. These processes include the transport of electrons through the conductors, the transport of protons through the electrolyte, the transfer of electrons or ions at the electrode–electrolyte interfaces, and kinetic losses. Measuring impedance spectra of fuel cell stacks the electrical engineer observes resistive, capacitive and inductive effects. Resistive effects can be assigned to the charge transfer and ohmic voltage losses of electron and proton conduction. Capacitive effects occur due to the double layers of electrode–electrolyte interfaces. The dynamics of mass transport acts as a first-order lag element. Inductive effects appear due to the inductance of the cables.

Therefore, the purpose of an application-oriented impedance characterisation of a fuel cell stack during operation cannot be to reproduce the microscopic effects, especially not at very high or very low frequencies. The purpose of the presented method is to determine the essential properties and loss factors of the fuel cell stack, their interrelations and their dependence on controllable variables as humidification, temperature, pressure and current. Thereby, it is virtually always assumed that the properties of the electrode-material system are time-invariant [2].

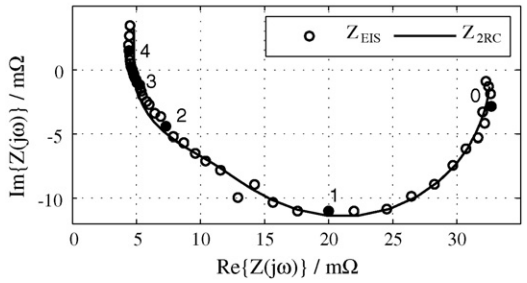

Fig. 1. Impedance spectrum of a PEM fuel cell stack, five cells, $A = 100\,\mathrm{cm}^2$ at $\lambda_C = 3.33$ and $\lambda_A = 1.25$, $i_{FC} = 0.8\,\mathrm{A\,cm}^{-2}$, $T_{Stack} = 55\,^{\circ}\mathrm{C}$, $T_{DP} = 50\,^{\circ}\mathrm{C}$, $p_A = 1\,\mathrm{bar_{abs}}$, $p_C = 1\,\mathrm{bar_{abs}}$, $f_{min} = 0.5\,\mathrm{Hz}$, solid symbols denote decades of frequency.

2.2. Impedance model

The goal of impedance modelling is to find a model with a concise mathematical structure which regards the dominant effects and reflects the essential properties of the electrochemical system. To enable an interpretation of the model parameters and to guarantee a comparability of identified impedance spectra, the impedance model should include a minimum number of parameters and should yield a minimum error in between the model output and the measurement.

Fig. 1 shows a typical impedance spectrum of a polymer electrolyte fuel cell (PEMFC). It is the Nyquist plot of a five cell stack with an active surface of $100\,\mathrm{cm}^2$, a commercially available membrane electrode assembly with Pt/Ru and the gas diffusion layer SGL 10BB. The spectrum was measured at a current density of $0.8\,\mathrm{A\,cm}^{-2}$ with a minimum frequency of $f_{min} = 0.5\,\mathrm{Hz}$, and a maximum frequency of $f_{max} = 10\,\mathrm{kHz}$.

In general, the impedance of a PEMFC can be depicted as an equivalent circuit of an ohmic resistance R_Ω and two impedances Z_1 and Z_2 for the two loops in the Nyquist plot. Whereby the firs loop at low frequencies can primarily be assigned to kinetic losses and the double layer, and the second loop at higher frequencies to transport phenomena. The resulting fuel cell impedance is

$$Z_{FC}(j\omega) = R_\Omega + Z_1(j\omega) + Z_2(j\omega) \quad (1)$$

The intersection of the frequency response locus in Fig. 1 with the real axis at $\omega \to \infty$ corresponds to the ohmic resistance R_Ω. The intersection of the frequency response locus with the real axis at $\omega = 0$ corresponds to the sum of resistances $R_\Sigma = R_\Omega + R_1 + R_2$, where R_1 and R_2 are the limit values of Z_1 and Z_2 for $\omega \to 0$. The diverging impedance for $\omega \to \infty$ mainly results from the inductance L of the cables, which is not part of the fuel cell impedance. In the fuel cell impedance model (2RC-model) depicted in Fig. 2, the losses of the electron and proton conductance are described by an ohmic resistance and the two loops of the impedance spectrum each by an *RC*-circuit [3,12,13]. In the frequency domain the impedance of

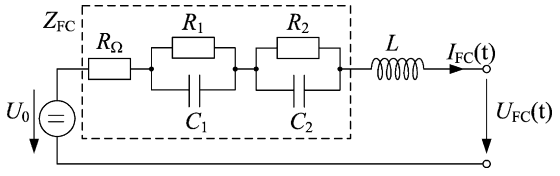

Fig. 2. Model of the fuel cell impedance with voltage source and cable inductance.

the 2*RC*-model in Fig. 2 is

$$Z_{2RC}(j\omega) = R_\Omega + Z_{RC_1}(j\omega) + Z_{RC_2}(j\omega) = R_\Omega + \frac{R_1}{1+j\omega\tau_1} + \frac{R_2}{1+j\omega\tau_2} \quad (2)$$

with the time constants $\tau_1 = R_1C_1$ and $\tau_2 = R_2C_2$ of the two *RC*-circuits.

This two time constants model has its limitations, e.g., when one limiting process is diffusion-based, but it is sufficient for the present introduction of the identification method. More complex impedance models, e.g., with distributed time constants [14,15] would presumably yield better fits to the impedance spectra but shall not be regarded here because of the complexity of fractional calculus.

2.3. Electrochemical parameter identification

The goal of EPI is to identify the parameters of the transformed impedance model directly on basis of the time response of the fuel cell to an excitation, instead of on basis of the impedance spectrum. Basis of the method is that the time response of an appropriately perturbed fuel cell incorporates the same information on the impedance of the system as the frequency response, so that the impedance can be calculated from the perturbation and response in the time domain [11].

The process flow of the electrochemical parameter identification is composed of:

1. Excitation of the system.
2. Measurement of the fuel cell current and voltage.
3. Digital signal processing for noise reduction and offset adjustment.
4. Parameter optimisation by minimising the error between the measured and modelled system response.

The single steps will be discussed in the following sections.

2.4. Model transformation into time domain

The general prerequisite for the application of the electrochemical parameter identification is the existence of an appropriate model and the ability to transform this model, at least approximately, into time domain.

For the use in the time domain the equivalent circuit of the fuel cell model comprises the impedance and a constant voltage source (equilibrium voltage) U_0 (Fig. 2). Thereby, the fuel cell impedance acts as the internal resistance of the voltage source. Thus, the time domain model incorporates both the loss factors and the source terms of the fuel cell stack. For time domain measurements the cable inductance can be neglected. In the time domain the model can be expressed mathematically by real-valued, algebraic equations for Kirchhoff's voltage law (3) and Ohm's law (4) as well as two ordinary differential equations (5) and (6) for the voltage drop at the two *RC*-circuits:

$$U_{FC}(t) = U_0 - U_\Omega(t) - U_1(t) - U_2(t) \quad (3)$$

$$U_\Omega(t) = R_\Omega I_{FC}(t) \quad (4)$$

$$\tau_1 \frac{d}{dt}U_1(t) + U_1(t) = R_1 I_{FC}(t) \quad (5)$$

$$\tau_2 \frac{d}{dt}U_2(t) + U_2(t) = R_2 I_{FC}(t) \quad (6)$$

The measured signals of the excitation I_{FC} and the system response U_{FC} are sampled at a constant rate (sampling time T). And "since the world of electrochemistry is an analog one, the use of digital computation methods must be preceded by analog-to-digital conversion " [11]. Hence Eqs. (3)–(6) have to be discretised for the application in the identification algorithm. The differential equations (5) and (6) are thereby transformed approximately into the difference equations:

$$U_{1,k} = f_1(I_{FC,k}, I_{FC,k-1}, U_{1,k-1}) \quad (7)$$

and

$$U_{2,k} = f_2(I_{FC,k}, I_{FC,k-1}, U_{2,k-1}) \quad (8)$$

where k is the discrete time index. In the following, gathered values for the fuel cell current $I_{FC,k}$ and for the voltage $U_{FC,k}$ at the discrete time steps $t = kT$ are presented as the data vectors $\underline{I}_{FC}$ and $\underline{U}_{FC}$. The parameters which have to be identified are combined in the parameter vector $\underline{\theta} = [R_\Omega R_1 R_2 C_1 C_2 U_0]^T$.

Since the same impedance parts (resistances and capacitances) are identified, EPI extracts the same information from the fuel cell impedance as EIS does and additionally the voltage source of the stack. Concerning the validity of the model it has to be stated that for both the model in frequency and in time domain the structure of the model can be used over the whole range of the IV-characteristics; but the parameters are only valid in a neighbourhood of the operating point.

2.5. Excitation signal generation

As in EIS, the fuel cell current and voltage at an operating point consist of a constant and a superimposed time-varying part:

$$I_{FC}(t) = I_{dc} + I_{ac}(t) \quad (9)$$

$$U_{FC}(t) = U_{dc} + U_{ac}(t) \quad (10)$$

At EPI the fuel cell current acts as the input signal and the fuel cell voltage as the system response. Finally, the goal of the parameter optimisation is to minimise the error:

$$\underline{e}(\underline{\theta}) = \underline{U}_{FC} - \underline{U}_{FC,mod}(\underline{\theta}) \quad (11)$$

between points in the measured data vector U_{FC} and corresponding points generated by the fuel cell model $\underline{U}_{FC,mod}(\underline{\theta})$ for the given input sequence $\underline{I}_{FC}$. Hence, the objective function $J(\underline{\theta})$ is defined as the sum of the squares of the residuals:

$$J(\underline{\theta}) = \underline{e}^T(\underline{\theta})\underline{e}(\underline{\theta}) = \Sigma_\kappa(e_k(\underline{\theta}))^2 \quad (12)$$

In order to identify a parameter by minimising the objective function the input signal has to excite the part of the system which is described by this parameter. Or reverse, the parameter has to have an influence on the model output and thereby on the objective function at a defined input sequence. A measure of the influence of a parameter is its sensitivity. Here, sensitivity describes the effect of an arbitrary parameter variation of a single parameter on the output function [16]. Thereby, the sensitivity analysis compares the model output at nominal parameter values $U_{FC,mod}(\underline{\theta}_{FC})$ with the model output $U_{FC,mod}(\underline{\theta}_{var})$ for a parameter variation $\Delta\theta_i$ of a single parameter θ_i. Accordingly, for EPI the sensitivity of a parameter θ_i is defined as

$$S(\Delta\theta_i) = \underline{e}^T(\Delta\theta_i)\underline{e}(\Delta\theta_i) \quad (13)$$

with

$$\underline{e}(\Delta\theta_i) = \underline{U}_{FC,mod}(\underline{\theta}_{FC}) - \underline{U}_{FC,mod}(\underline{\theta}_{var}) \quad (14)$$

The sensitivity of the parameters can be used to find the appropriate excitation signal [17].

In general, excitation signals can be any arbitrary function of time [11]. But some constraints have to be regarded. On the one

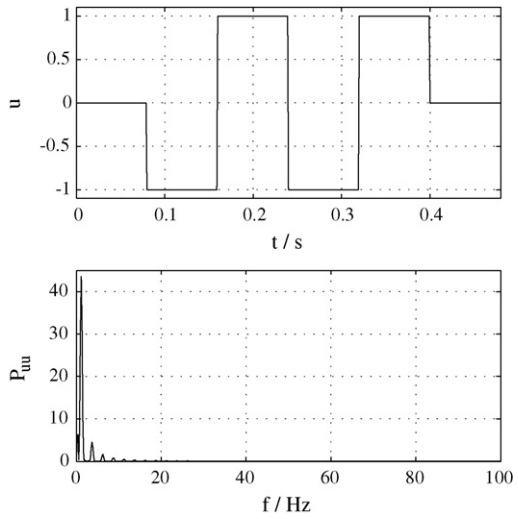

Fig. 3. Rectangular signal and discrete power density spectrum of the rectangular signal at a sampling time of $T = 1$ ms.

hand it is crucial to keep the perturbation amplitude sufficiently small in order to be able to neglect nonlinear effects [3]. On the other hand the amplitude must not be too small to guarantee a minimum signal to noise ratio of the system response. Appropriate excitation signals are sinusoidal signals, step and rectangular, and noise functions. A chirp signal is a special sinusoidal signal with a linearly or exponentially time-dependent frequency $\omega(t)$:

$$x_{\text{chirp}}(t) = A\sin(\omega(t)t). \tag{15}$$

Regarding their power density spectra these signals differ significantly from each other. Figs. 3 and 4 show two potential excitation signals $u(t)$ and their discrete power density spectra $P_{uu}(f)$ at a sampling time of $T = 1$ ms. Whereas the discrete power density of the rectangular signal has a high peak at a low frequency, peaks with exponentially decreasing height at increasing frequencies and in between frequency ranges with a power density of zero, the exponential chirp signal shows a more uniformly distributed power density in the frequency range of the chirp signal. A combination of both signals leads to a signal with stationary parts and a power

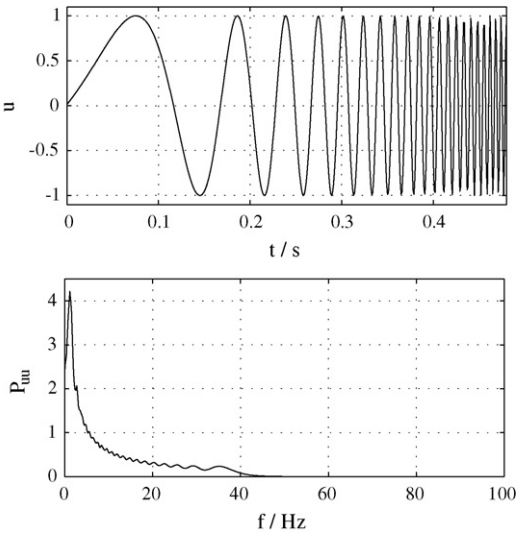

Fig. 4. Exponential chirp signal and discrete power density spectrum of the exponential chirp signal at a sampling time of $T = 1$ ms.

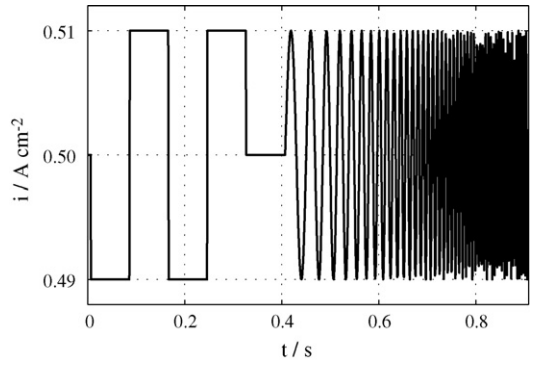

Fig. 5. Fuel cell current density as excitation signal, $i_{\text{amp}} = 0.01\ \text{A cm}^{-2}$, pulse width $\Delta T = 0.08$ s, chirp frequencies $f_{\min} = 2$ Hz, $f_{\max} = 50$ Hz.

density always unequal to zero for all frequencies in the range of the chirp signal.

These considerations together with the analysis of the sensitivity of the combined signal [17] lead to the appropriate excitation current density signal in Fig. 5 for the examined fuel cell stack. It has an alternating current signal amplitude of $i_{\text{amp}} = 0.01\ \text{A cm}^{-2}$, a pulse width of 0.08 s, a minimum chirp frequency of $f_{\min} = 2$ Hz, and a maximum chirp frequency of $f_{\max} = 50$ Hz. The choice of the signal parameters as pulse width and frequencies are strongly related to the expected time constants of the *RC*-circuits and thus on the analysed fuel cell stack.

2.6. Parameter optimisation algorithm

The task of the optimisation algorithm is to extract the information on the impedance which is incorporated in the excitation signal and the system response, by identifying the optimal set of parameters which characterise the fuel cell impedance and the voltage source. The optimal parameter vector $\underline{\theta}^*$ minimises the real-valued objective function (12). The search space of the parameters is constrained by a lower bound $\underline{\theta}_{\text{lb}}$ and an upper bound $\underline{\theta}_{\text{ub}}$ (see Table 1) given by expert knowledge and physical constraints as positive values for resistances, capacitances, and time constants. The difficulty and the challenge of determining the optimal parameter vector in the time domain is referred to the fact that the objective function is a multiminima function where beside the global minimum several local minima may exist. Therefore a hybrid optimisation algorithm consisting of a stochastic and a deterministic method is applied. Stochastic methods are mostly better suited to find the global optimum of multiminima functions, but on their own they show slow convergence properties. Deterministic methods show fast convergence properties, but often do not have the ability to overcome local minima. A hybridisation provides the possibility to combine the advantages of both types of methods [18]. The stochastic method applied is an evolutionary algorithm [19,20] and the deterministic method the downhill simplex method of Nelder and Mead [21].

Table 1
Nominal parameter vector θ_{FC}, boundaries of the search space: lower bound $\underline{\theta}_{\text{lb}}$ and upper bound $\underline{\theta}_{\text{ub}}$

	$\underline{\theta}_{\text{lb}}$	$\underline{\theta}_{\text{FC}}$	$\underline{\theta}_{\text{ub}}$
R_Ω (mΩ)	3	6.8	10
R_1 (mΩ)	4	6.5	30
R_2 (mΩ)	5	8.3	30
C_1 (F)	1	3.6	20
C_2 (F)	0.1	0.38	2
U_0 (V)	4	4.2	6

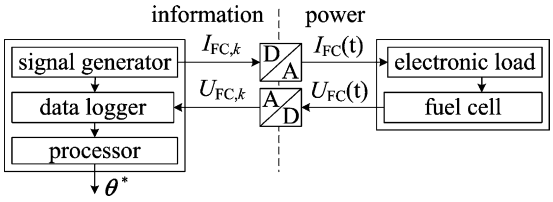

Fig. 6. Measurement setup and data processing of the EPI.

The evolutionary algorithm performs the task of the global search. It is terminated when the region of attraction of the global minimum is reached and passes its best parameter vector to the deterministic local search. In the hybrid algorithm the Nelder–Mead method performs the task of the local search for the final convergence towards the global minimum. Both parts of the hybrid algorithm perform a constrained optimisation regarding the bounds of the search space. Both are terminated by a maximum number of iterations to guarantee a maximum computing time. Ultimately the convergence to the global minimum cannot be proven, but repeated experiments have yielded reliable and reproducible results.

To increase the accuracy and reliability of the electrochemical parameter identification the method can be provided with redundancy. For this purpose subsequent signal sequences (time-frames of the signals) can be optimised independently. Finally the parameter vector with the lowest value of the objective function can be selected or the optimised parameter vectors can be averaged. This parallel optimisation of several signal sequences leads to an increased measurement and calculation time. If the application is critical in terms of time it is sufficient to optimise just one signal sequence.

2.7. Hardware setup and digital signal processing

The hardware setup of the electrochemical parameter identification (Fig. 6) consists of standard hardware components: a signal generator for the excitation signal, a data logger for the input and output signals, a processor for the parameter optimisation, and the D/A and A/D converters for the transition between the analogue and the discrete world. EPI works without the need of a frequency analyser.

For a reliable parameter optimisation the input signal of the system model should be as free of noise as possible. A noisy signal as input of the difference equation would otherwise lead to a disturbed output signal and finally to shifted minima of the objective function. Simple low-pass filtering could be problematic if the frequency range of the noise overlaps with the frequency range of the excitation signal. Therefore, the noise-free data of the signal generator is used as input of the optimisation algorithm instead of the measured fuel cell current at the electronic load. To adjust the values of the signal generator to the measured values the offset is corrected by averaging and the gain (amplitude of the superimposed small signal) is optimised using the golden section optimisation algorithm [22] which is an efficient line search algorithm.

3. Results

The electrochemical parameter identification was intensively tested for various operation conditions (variation of pressure, temperature, current density, humidification, hydrogen and oxygen excess ratio) of the fuel cell stack. Figs. 7 and 8 show the fuel cell response $U_{FC}(t)$ to the same input signal of Fig. 5, the first at a oxygen excess ratio of $\lambda_C = 5$ and a hydrogen excess ratio of $\lambda_A = 1.43$,

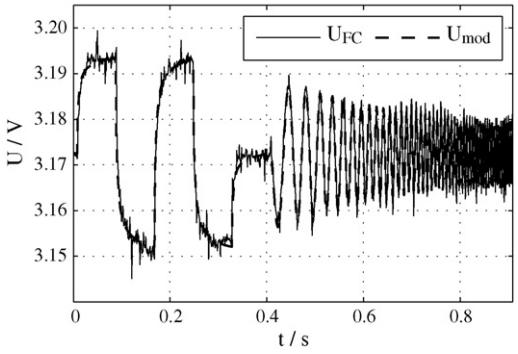

Fig. 7. Fuel cell stack voltage as system response to the excitation signal at $\lambda_C = 5$ and $\lambda_A = 1.43$, PEM fuel cell stack, five cells, $A = 100\,cm^2$, constant operation conditions: $i_{FC} = 0.5\,A\,cm^{-2}$, $T_{Stack} = 55\,^\circ C$, $T_{DP} = 50\,^\circ C$, $p_A = 1\,bar_{abs}$, $p_C = 1\,bar_{abs}$.

the second at $\lambda_C = 2.5$ and $\lambda_A = 1.11$. All other controllable variables as temperature, humidification, current density and pressure are kept constant. Figs. 7 and 8 additionally show the corresponding model outputs $U_{FC,mod}(t)$ which are calculated using the optimised parameter vector $\underline{\theta}^*$. The sampling time T of both signals is 1 ms. The transient response to the current steps, the amplitude and the increasing damping of the chirp signal, as well as the DC offset are characteristic for the impedance of the examined fuel cell stack. Together they incorporate sufficient information for the identification of the parameters.

If a single signal sequence as depicted in Figs. 7 and 8 is used for the optimisation the measurement time equals the length of the signal sequence $T_m = 0.91$ s. The calculation time of a standard computer needed for the digital signal processing and the parameter optimisation is $T_c = 1.25$ s. In case of a parallel optimisation of five subsequent signal sequences the measurement time increases by a factor of 5 to $T_m = 4.55$ s, the calculation time increases to $T_c = 6.11$ s. The standard computer used is defined by the following software and hardware features: Matlab 7.1, Windows XP, Intel Pentium M 1.6 GHz, 0.99 GB RAM.

For a verification of the identification process of EPI and a validation of the results, reference measurements at the same operation conditions were taken in the frequency domain (Figs. 9 and 10) and analysed using the electrochemical impedance spectroscopy. On the basis of the impedance spectra the parameters of the impedance model were identified and can now be compared directly with the according parameters of the time domain model.

To get an optical impression of the agreement of both identified models a virtual frequency response is calculated using

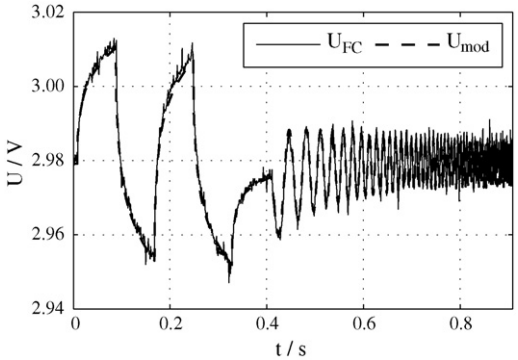

Fig. 8. Fuel cell stack voltage as system response to the excitation signal at $\lambda_C = 2.5$ and $\lambda_A = 1.11$, PEM fuel cell stack, five cells, $A = 100\,cm^2$, constant operation conditions: $i_{FC} = 0.5\,A\,cm^{-2}$, $T_{Stack} = 55\,^\circ C$, $T_{DP} = 50\,^\circ C$, $p_A = 1\,bar_{abs}$, $p_C = 1\,bar_{abs}$.

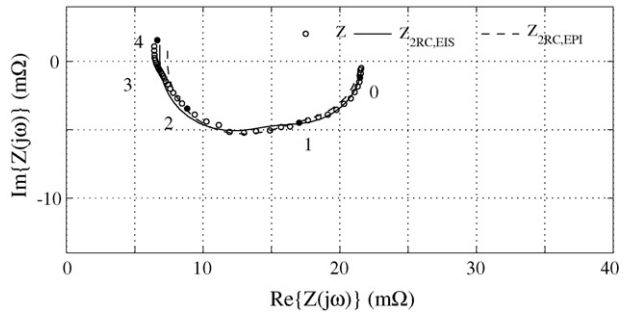

Fig. 9. Comparison of measured and modelled impedance spectra at $\lambda_C = 5$ and $\lambda_A = 1.43$, PEM fuel cell stack, five cells, $A = 100\,cm^2$, constant operation conditions: $i_{FC} = 0.5\,A\,cm^{-2}$, $T_{Stack} = 55\,^\circ C$, $T_{DP} = 50\,^\circ C$, $p_A = 1\,bar_{abs}$, $p_C = 1\,bar_{abs}$, $f_{min} = 0.5$ Hz, solid symbols denote decades of frequency.

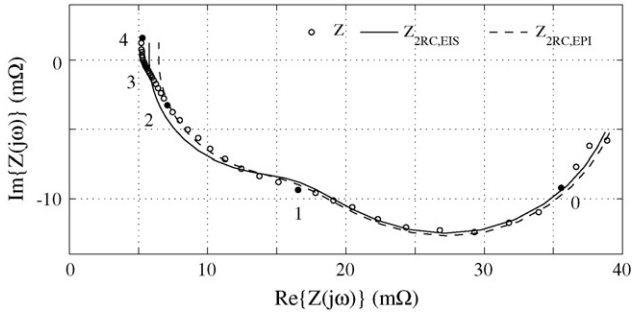

Fig. 10. Comparison of measured and modelled impedance spectra at $\lambda_C = 2.5$ and $\lambda_A = 1.11$, PEM fuel cell stack, five cells, $A = 100\,cm^2$, constant operation conditions: $i_{FC} = 0.5\,A\,cm^{-2}$, $T_{Stack} = 55\,^\circ C$, $T_{DP} = 50\,^\circ C$, $p_A = 1\,bar_{abs}$, $p_C = 1\,bar_{abs}$, $f_{min} = 0.5$ Hz, solid symbols denote decades of frequency.

the impedance parameters identified in the time domain. In Figs. 9 and 10 the frequency responses of the impedance model of both identified parameter vectors is plotted for the same frequency range next to the measured impedance spectra.

It is obvious that the impedance has changed dramatically between the different operation conditions. For both extremely different settings EPI was able to identify the impedance parameters. Both Nyquist plots show that the impedance spectra Z_{EPI}, with the parameters identified in the time domain show a very good agreement with the measured impedance spectra, especially for small and intermediate frequencies (0.5 Hz to 0.5 kHz). For high frequencies the virtual impedance spectra Z_{EPI} slightly diverge from the measured spectra which lead to an overestimation of the ohmic resistances. The according values of the parameters and the corresponding values of the objective function are listed in Table 2. Whereby the objective function of the impedances is defined as

$$J(\underline{\theta}) = \Sigma_\kappa (g_R e_{R,k}(\underline{\theta}))^2 + \Sigma_\kappa (g_I e_{I,k}(\underline{\theta}))^2 \tag{16}$$

Table 2
Comparison of the identified fuel cell impedance parameters at different excess ratios with corresponding values of the objective function

	$\lambda_C = 5$, $\lambda_A = 1.43$		$\lambda_C = 2.5$, $\lambda_A = 1.11$	
	EIS	EPI	EIS	EPI
R_Ω (mΩ)	6.84	7.39	5.77	6.47
R_1 (mΩ)	6.54	5.00	22.9	23.2
R_2 (mΩ)	8.26	9.02	11.2	10.5
C_1 (F)	3.61	5.28	3.19	3.13
C_2 (F)	0.38	0.45	0.59	0.69
$J(\underline{\theta})$	6.7 e−6	1.6 e−5	1.7 e−5	2.7 e−5

with the errors of the real and the imaginary part:

$$e_R(\underline{\theta}) = Re\{Z_{FC}(j\omega)\} - Re\{Z_{FC,mod}(j\omega)\} \text{ and}$$
$$e_I(\underline{\theta}) = Im\{Z_{FC}(j\omega)\} - Im\{Z_{FC,mod}(j\omega)\} \tag{17}$$

and the corresponding weight factors $g_R = 1$ and $g_I = 2$.

4. Conclusion

Electrochemical parameter identification is – in terms of measurement time and costs for hardware – an efficient method for fuel cell impedance characterisation, which works without additional sensors and less interference to the fuel cell operation than other time domain methods. EPI identifies the impedance parameters at different operating conditions reliably and reproducibly. The accuracy of the identified parameters is slightly lower than when EIS is applied. The membrane resistance is identified with an appraisable overestimation of about 5–10%. The biggest advantage of EPI is the short measurement time of 1–5 s, in comparison to 3–10 min for EIS, and the short calculation time of 1–7 s. Additionally, the waiting time to reach a drift-free working point is drastically reduced. Since only short signal sequences need to be analysed, EPI is applicable to online operation. The user can poll information on the current state of the fuel cell more often and during operation. In terms of costs of hardware, EPI is cheaper and simpler, because it does not need a frequency analyser.

As mentioned earlier, the main shortcoming is the simple impedance model used. This needs to be addressed in future work by applying more complex models to the identification procedure. Another limitation is the applied frequency range. As shown in the compared impedance spectra of Figs. 9 and 10 the models identified in time domain show good agreement with the measured impedance spectra in the applied frequency range of $f = 0.5$ Hz–10 kHz. Beyond this range no statements can be made.

For EPI a multitude of possible applications open up. The first field of applications is that of analysis and diagnosis of fuel cells, and especially the detection of malfunctions and errors. Continuous information on the parameters and the change of these parameters over time can be used to analyse the processes taking place in the cell, e.g., reaction kinetics and kinetic hindrances, diffusion effects as well as the water uptake of the membrane [7]. Another feature of the online identification of fuel cell parameters is detailed statistics and documentation, especially at lifetime experiments or long-term observation on aging and degeneration effects. By recording the single loss and source terms of the fuel cell model, the developer has much more information on the fuel cell than just recording static voltage and current values. Furthermore, EPI enables the user to monitor the fuel cell stack and single cells in parallel, due to the fact that measuring multiple voltage signals does not require a major additional effort.

The second field of applications is the balance of plant. The parameters of the fuel cell model identified at regular intervals provide a deeper insight in the current state of the fuel cell stack. The information on single loss terms opens the possibility of specific and focused measures for minimising these losses and increasing the efficiency of the fuel cell system. For example, the observation of an increasing transport resistance provides an indication of flooding in the GDL which can be responded by purging or a change of the gas flow to carry out liquid water. The second example again is tightly linked to the crucial task of water management of a fuel cell: the measurement of the membrane resistance by EPI enables a closed loop for the humidification control and decreases thereby the risk of membrane drying and flooding of the gas diffusion layer. Finally, EPI can make a contribution to increase the efficiency, durability, and dynamics of fuel cell systems.

Acknowledgement

The authors gratefully acknowledge the cooperation and support by the Center for Solar Energy and Hydrogen Research (ZSW) in Ulm, especially for the opportunity of using their test environment.

References

[1] B.H. Andreaus, Die Polymer-Elektrolyt-Brennstoffzelle-Charakterisierung ausgewählter Phänomene durch elektrochemische Impedanzspektroskopie (German), Ph.D. Thesis, EPF Lausanne, Switzerland, 2002.
[2] J.R. Macdonald, W.B. Johnson, Impdedance Spectroscopy—Theory, Experiment, and Applications, John Wiley & Sons, 2005, pp. 1–26.
[3] E. Ivers-Tiffée, A. Weber, H. Schichlein, Handbook of Fuel Cells—Fundamentals, Technology and Applications, John Wileys & Sons, 2003, pp. 220–235.
[4] A. Lasia, Electrochemical Impedance Spectroscopy and its Applications, Kluwer Academic, 1999, pp. 143–248.
[5] A. Hakenjos, Untersuchung zum Wasserhaushalt von Po-ly-mer-elek-trolyt-mem-bran-Brenn-stoff-zel-len (German), Ph.D. Thesis, Albert-Ludwig University Freiburg, Germany, 2006.
[6] H. Kuhn, In-Situ Charakterisierung von Polymer-Elektrolyt Brennstoffzellen mittels Elektrochemischer Impedanzspektroskopie (German), Ph.D. Thesis, ETH Zürich, Switzerland, 2006.
[7] J. Le Canut, R.M. Abouatallah, D.A. Harrington, J. Electrochem. Soc. 153 (2006) A857–A864.
[8] N. Wagner, J. Appl. Electrochem. 32 (2002) 859–863.
[9] F. Richter, C. Schiller, N. Wagner, Electrochemical Applications—Advances in Electrochemical Applications of Impedance Spectroscopy, Zahner-Elektrik, 2002.
[10] L. Schindele, Einsatz eines leistungselektronischen Stellglieds zur Parameteridentifikation und optimalen Betriebsführung von PEM-Brennstoffzellensystemen (German), Ph.D. Thesis, University Karlsruhe, Germany, 2006.
[11] M.C.H. McKubre, D.D. Macdonnald, Impedance Spectroscopy—Theory, Experiment and Applications, John Wiley & Sons, 2005, pp. 129–167.
[12] C.H. Hamann, W. Vielstich, Elektrochemie (German), Wiley–VCH Verlag, 1998.
[13] J.E. Bauerle, J. Phys. Chem. Solids 30 (1969) 2657–2670.
[14] A. Sadkowski, Electrochim. Acta 38 (1993) 2051–2054.
[15] M. Haschka, B. Rüger, V. Krebs, A. Weber, V. Sonn, E. Ivers-Tiffée, Proceedings of the European SOFC Forum 2004, Lucerne, Switzerland, 2004, pp. 557–568.
[16] S.S. Isukapalli, Uncertainty Analysis of Transport-Transformation Models, Ph.D. Thesis, State University of New Jersey, USA, 1999.
[17] M.A. Danzer, U. Berndgen, M. Wegscheider, E.P. Hofer, Proceedings of Hydrogen and Fuel Cells 2007, Vancouver, Canada, 2007.
[18] R. Chelouah, P. Siarry, Eur. J. Oper. Res. 148 (2003) 335–348.
[19] J. Holland, SIAM J. Comput. 2 (1973) 88–105.
[20] I. Rechenberg, Evolutionsstrategie: Optimierung technischer Systeme nach Prinzipien der biologischen Evolution (German), Frommann Holzboog (1973).
[21] J. Nelder, R. Mead, Comput. J. 7 (1965) 308–313.
[22] J. Kiefer, Proc. Am. Math. Soc. (1953) 502–506.